

Association of Bergmeister Papilla and Deep Optic Nerve Head Structures With Prelaminar Schisis of Normal and Glaucomatous Eyes



HITOMI SAITO, TAKASHI UETA, MAKOTO ARAIE, NOBUKO ENOMOTO, MITSUKI KAMBAYASHI, HIROSHI MURATA, TSUTOMU KIKAWA, KAZUHISA SUGIYAMA, TOMOMI HIGASHIDE, ATSUYA MIKI, AIKO IWASE, GOJI TOMITA, TORU NAKAZAWA, MAKOTO AIHARA, KYOKO OHNO-MATSUI, TAE-WOO KIM, CHRISTOPHER KAI SHUN LEUNG, LINDA M. ZANGWILL, AND ROBERT N. WEINREB

PURPOSE: To investigate factors associated with the severity of prelaminar schisis (PLS) in healthy subjects and glaucoma patients.

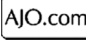
DESIGN: Prospective cross-sectional study.

METHODS: A total of 217 eyes of 217 subjects (110 normal eyes and 107 open angle glaucoma eyes) were studied. Frequency and severity of PLS were compared between normal and glaucomatous eyes. Multivariate logistic models were used to assess factors associated with the severity of PLS. Factors considered were age, axial length, glaucomatous damage indices, Bruch membrane opening (BMO) and anterior scleral canal opening parameters, tractional forces (posterior vitreous staging and presence of Bergmeister papilla), circumpapillary choroidal thickness, lamina cribrosa (LC) parameters, and peripapillary scleral (PPS) angle.

RESULTS: The frequency of PLS was 70.9% in normal eyes and 72.0% in glaucomatous eyes. There was no difference in frequency and severity between the groups.

The presence of Bergmeister papilla was the strongest predictor of a more severe PLS in both normal and glaucomatous eyes (odds ratio [OR] + 9.78, 12.5; both $P < .001$). A larger PPS angle in normal eyes (OR = 1.19; $P = .003$) and a larger BMO area and a deeper LC depth in glaucomatous eyes (OR = 1.08, 1.05; both $P = .038$) were associated with severity of PLS.

CONCLUSIONS: The severity of PLS was strongly associated with the presence of Bergmeister papilla, suggesting a traction-related phenomenon. Correlation of PLS severity with larger BMO area and deeper LC depth, which are optic nerve head structures associated with glaucoma, suggested its possible relationship with glaucomatous damage. (Am J Ophthalmol 2024;257: 91–102. © 2023 The Author(s). Published by Elsevier Inc. This is an open access article under the CC BY-NC-ND license (<http://creativecommons.org/licenses/by-nc-nd/4.0/>))

 Supplemental Material available at AJO.com.
Accepted for publication September 1, 2023.

From the Department of Ophthalmology (H.S., T.U., M.K., M.A.), Graduate School of Medicine, The University of Tokyo, Tokyo, Japan; Kanto Central Hospital of the Mutual Aid Association of Public School Teachers (M.A.), Tokyo, Japan; Tokyo Teishin Hospital (N.E.), Tokyo, Japan; Center Hospital of the National Center for Global Health and Medicine (H.M.), Tokyo, Japan; R&D Division (T.K.), Topcon Corporation, Tokyo, Japan; Department of Ophthalmology (K.S., T.H.), Kanazawa University Graduate School of Medical Sciences, Kanazawa, Japan; Department of Innovative Visual Science (A.M.), Osaka University Graduate School of Medicine, Osaka, Japan; Department of Myopia Control Research (A.M.), Aichi Medical University Medical School, Nagakute, Japan; Tajimi Iwase Eye Clinic (A.I.), Tajimi, Japan; Department of Ophthalmology (G.T.), Toho University Ohashi Medical Center, Tokyo, Japan; Department of Ophthalmology (T.N.), Graduate School of Medicine, Tohoku University, Sendai, Japan; Department of Ophthalmology and Visual Science (K.O.-M.), Tokyo Medical and Dental University, Tokyo, Japan; Department of Ophthalmology (T.-W.K.), Seoul National University College of Medicine, Seoul National University Bundang Hospital, Seongnam, Korea; Department of Ophthalmology (C.K.S.L.), LKS Faculty of Medicine, the University of Hong Kong, Hong Kong Special Administrative Region, China; Hamilton Glaucoma Center (L.M.Z., R.N.W.), Shiley Eye Institute, and the Viterbi Family Department of Ophthalmology, University of California San Diego, La Jolla, California, USA
Inquiries to Hitomi Saito, Graduate School of Medicine, University of Tokyo, Tokyo, Japan; e-mail: hitomi8678@gmail.com

EVALUATION OF THE INTRA-OPTIC DISC REGION including the lamina cribrosa (LC) and peripapillary sclera (PPS) is of special interest, because these regions are considered to be the primary site of damage in open-angle glaucoma (OAG).¹⁻⁴ The advancement of optical coherence tomography (OCT) technology has enabled visualization of microstructures of the optic nerve head (ONH) that are not observed otherwise, providing new insights into ONH structural changes. Recently, a splitting or schisis-like deformation of the prelaminar tissue, prelaminar schisis (PLS), observed on spectral domain OCT (SD-OCT) images, was reported.⁵

A higher frequency and a more severe PLS in early glaucomatous eyes in comparison to normal eyes was found in a previous study.⁶ Deeper ONH cupping in normal and mildly glaucomatous eyes⁶ and deeper LC depth (LCD) in advanced glaucomatous eyes⁷ were associated with PLS. These studies implied that mechanical stress accompanying the deepening of ONH cupping may lead to a glial cell-induced disruption in prelaminar connective tissue. However, both studies^{6,7} failed to find a correlation between visual field indices and the presence or severity of PLS, render-

ing the relationship of PLS and glaucoma to be investigated further.

Although deepening of the ONH cup is one possible etiology for tissue disruption in the prelaminar region, the role of posterior vitreous traction and axial length (AXL) also need to be taken into consideration when considering retinal tissue splitting. Sung et al reported an association with shorter AXL and PLS in advanced glaucomatous eyes,⁷ suggesting the possibility of changes in posterior vitreous traction due to AXL-related vitreous liquification to be one factor associated with PLS. Furthermore, peripapillary retinoschisis, which is a similar disruption of the inner retinal layers outside the optic disc, is often associated with longer AXL and glaucoma,⁸⁻¹⁰ and similar associations may exist with intra-disc connective tissue disruptions.

The use of swept-source OCT (SS-OCT) enabling better visibility of the vitreo-retinal surface¹¹ may provide a deeper understanding of the factors associated with PLS. The purpose of this study is to further elucidate the clinical features of PLS using SS-OCT in normal and mild-to-moderate glaucomatous eyes without pathological myopia, taking possible involvement of ONH structure changes and tractional forces, including Bergmeister papilla and posterior vitreous detachment (PVD), into consideration.

METHODS

• **PARTICIPANTS:** Normal and glaucomatous subjects were recruited using identical inclusion criteria from 8 institutions (Kanazawa University, Kanto Central Hospital of the Mutual Aid Association of Public School Teachers, Osaka University, Tajimi Iwase Eye Clinic, Toho University Ohashi Medical Center, Tohoku University, University of Tokyo, Seoul National University Bundang Hospital, University of California San Diego, and Hong Kong Eye Hospital). Study protocols were approved by the institutional review board of Kanto Central Hospital (R1-06-005) and adhered to the tenets of the Declaration of Helsinki. All patients provided written informed consent before participation in the study.

Self-reported 30- to 70-year-old healthy volunteers and glaucoma patients were included. Ocular examinations, including refraction and corneal radius of curvature measurements (ARK-900; NIDEK), best-corrected visual acuity (BCVA) measurements with the 5-meter Landolt chart, AXL measurements (IOL Master; Carl Zeiss Meditec, Inc), slitlamp examination, intraocular pressure (IOP) measurements with Goldmann applanation tonometry, dilated funduscopy, fundus photography, stereophotography, and visual field testing with Humphrey Field Analyzer (HFA) 24-2 Swedish Interactive Threshold Algorithm Standard program (Carl Zeiss Meditec, Inc) were performed at the first visit.

Inclusion criteria for of this study were as follows: spherical equivalent (SE) of +1 diopter (D) or less, astigmatism <2 D, AXL <28 mm, BCVA >20/25, and attainment of good quality of OCT images and fundus photographs. Exclusion criteria are summarized in Table 1. If one eye of a subject met the exclusion criteria, both eyes were excluded from the study. One eye of each subject was randomly selected and enrolled in the study.

A normal eye had no abnormal findings upon complete ophthalmologic assessments, including slitlamp and fundus examinations, IOP <21 mm Hg, an open angle, normal optic disc appearance of both eyes based on clinical stereoscopic examination (by M.A., A.I., G.T., and K.O.M.), and normal HFA results.

A glaucomatous eye had an IOP of <21 mm Hg on the day of OCT measurements, an open angle, glaucomatous optic disc appearance based on clinical stereoscopic examination (by M.A., A.I., G.T., and K.O.M.), and abnormal HFA results with mean deviation greater than -12 dB corresponding to the optic glaucomatous changes. Abnormal HFA results were determined following criteria defined by the Hodapp–Parrish–Anderson criteria.¹²

• **SS-OCT MEASUREMENTS:** Details of OCT image acquisition and measurement of ONH structures have been reported previously.¹³ In brief, the ONH and macula of all subjects were imaged by a SS-OCT (DRI OCT Triton; Topcon, Inc). 6.0 x 6.0 mm ONH raster scans, 24-line Bruch membrane opening (BMO)-centered radial scans (8 B-scan averaging) and 12.0 x 9.0 mm wide raster scans including both the ONH and macula were obtained for each subject. Circumpapillary retinal nerve fiber layer thickness (cpRNFLT) and circumpapillary choroidal thickness (cpCHT) were measured upon a 3.4-mm-diameter BMO-centered annulus. The retinal pigment epithelium (RPE) edge, BMO, and anterior scleral canal opening (ASCO) were manually segmented on radial scans reconstructed from raster scans by 2 experienced examiners (H.S., M.K.) to calculate minimum rim width (MRW), BMO area/ovality, ASCO area/ovality, ASCO/BMO offset magnitude (representing the magnitude of ASCO centroid misalignment in reference to the BMO centroid),¹³ ASCO/BMO offset direction (representing the direction of misalignment of ASCO centroid in reference to the BMO centroid),¹³ and peripapillary atrophy (PPA)+BM/-BM. Magnification corrections were made using a modified Littmann equation¹⁴ provided by the manufacturer based on refractive error, corneal radius, and AXL.

Commercial artificial intelligence software, Reflectivity (Abyss Processing), was used for LC parameter measurements.^{5,15} LCD was defined as the distance between the BMO plane and anterior LC surface at the BMO center. Because the inner limiting membrane (ILM) is often elevated from the prelaminar surface in PLS eyes, we used LCD instead of ONH cup depth to assess the relationship between PLS and ONH cup depth.⁷ The LC global shape index (LC-

TABLE 1. Study Exclusion Criteria.

Contraindication to pupillary dilation
Narrow angle (Shaffer grade ≤ 2)
Unreliable HFA results (fixation loss or false negative $> 20\%$, false positive $> 15\%$)
Optic nerve or retinal abnormality other than glaucoma
Pathologically myopic eyes or its suspects (i.e. eyes with optic disc ovality > 1.33 upon fundus observation, inverted optic discs, posterior staphyloma, focal and/or diffuse macular chorioretinal atrophy, intrachoroidal cavitation, circular PPA zones)
History of intraocular or refractive surgery
Family history of glaucoma (normal subjects only)
History of ocular or systemic diseases that could affect HFA/OCT results.
(i.e. clinically significant cataract, diabetic retinopathy and/or maculopathy, age-related macular degeneration, epiretinal membrane)
History of systemic steroid or anti-cancer drugs, clinically significant hyper- or hypotension

HFA = Humphrey Field Analyzer; OCT = optical coherence tomography; PPA = peripapillary atrophy.

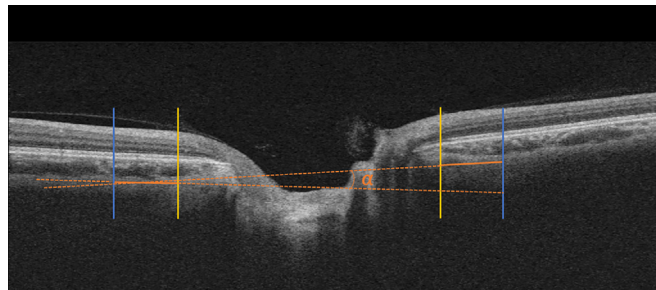


FIGURE 1. Illustration of measurement of peripapillary scleral (PPS) angle. The anterior scleral boundaries (orange solid line) are defined on the temporal and nasal side upon a single horizontal B-scan in the nasal-temporal direction between $1200 \mu\text{m}$ (yellow lines) and $1800 \mu\text{m}$ (blue lines) from the Bruch membrane opening center and then are extended (dotted orange line) until they intersect with each other. PPS angle (α) is defined as the angle between 2 extended anterior scleral boundaries. A larger angle represents a more posteriorly bowed v-shaped PPS configuration.

GSI) is an index with a numerical value between -1 and 1 quantifying the global shape of the LC anterior boundary.¹⁵ PPS angle quantifies the amount of PPS bowing and is defined as the angle between 2 lines parallel to the anterior scleral boundaries upon a single horizontal B-scan in the nasal-temporal direction (Figure 1). A larger angle represents a more posteriorly bowed v-shaped PPS configuration.^{5,16}

• **GRADING OF PLS ON OCT SCANS:** The 24-line BMO-centered radial scans were reviewed twice on independent occasions by one grader (H.S.) who was masked to all patient demographic, clinical, and ocular information. Any uncertain diagnosis was arbitrated by a separate observer (M.A.). Intra- and interobserver (H.S. and N.E.) reproducibility for detection of the presence and grading for PLS were determined on randomly selected 30 normal and 30 glaucomatous eyes from the cohort to ensure generalizability of the grader's decisions.

PLS was defined as the splitting of prelaminar tissue within the BMO boundary of the ONH observed in more than 2 consecutive radial scans. Involvement of retinal vessels being lifted or separated from the underlying prelaminar tissue was confirmed on all PLS eyes to ensure that the ob-

served void was not merely a space between an overlying membranous structure and the prelaminar tissue. PLS was further subdivided into 3 grades (grades 0, 1, 2) referencing the Lowry definition⁶ and taking involvement of retinal vessels into consideration (Figure 2). Eyes with grade 0 had no visible PLS. Eyes with grade 1 had relatively small optical voids mostly located between the ILM/meniscus of Kuhnt and anterior prelaminar tissue with voids surrounding the vessels. Eyes with grade 2 had larger and/or more deeply located voids with retinal vessels often lifted from the underlying prelaminar tissue. As there were only 3 eyes in the glaucoma group with grade 3 PLS with much larger schisis volume and definite disruption of the subsurface prelaminar tissue, those 3 eyes were included in grade 2 in our study for statistical purposes. Although PLS grading was conducted solely on the 24-line BMO-centered radial scans, all findings were confirmed on ONH raster scans to ensure that the minor splitting observed in eyes with grade 1 PLS were not OCT image artifacts.

• **EVALUATION OF POSTERIOR VITREOUS DETACHMENT:** Wide raster scans with vitreous visibility enhancement by the Enhanced Vitreous Visibility module¹⁷ were used for evaluation of PVD. Eyes with no PVD, separation of the

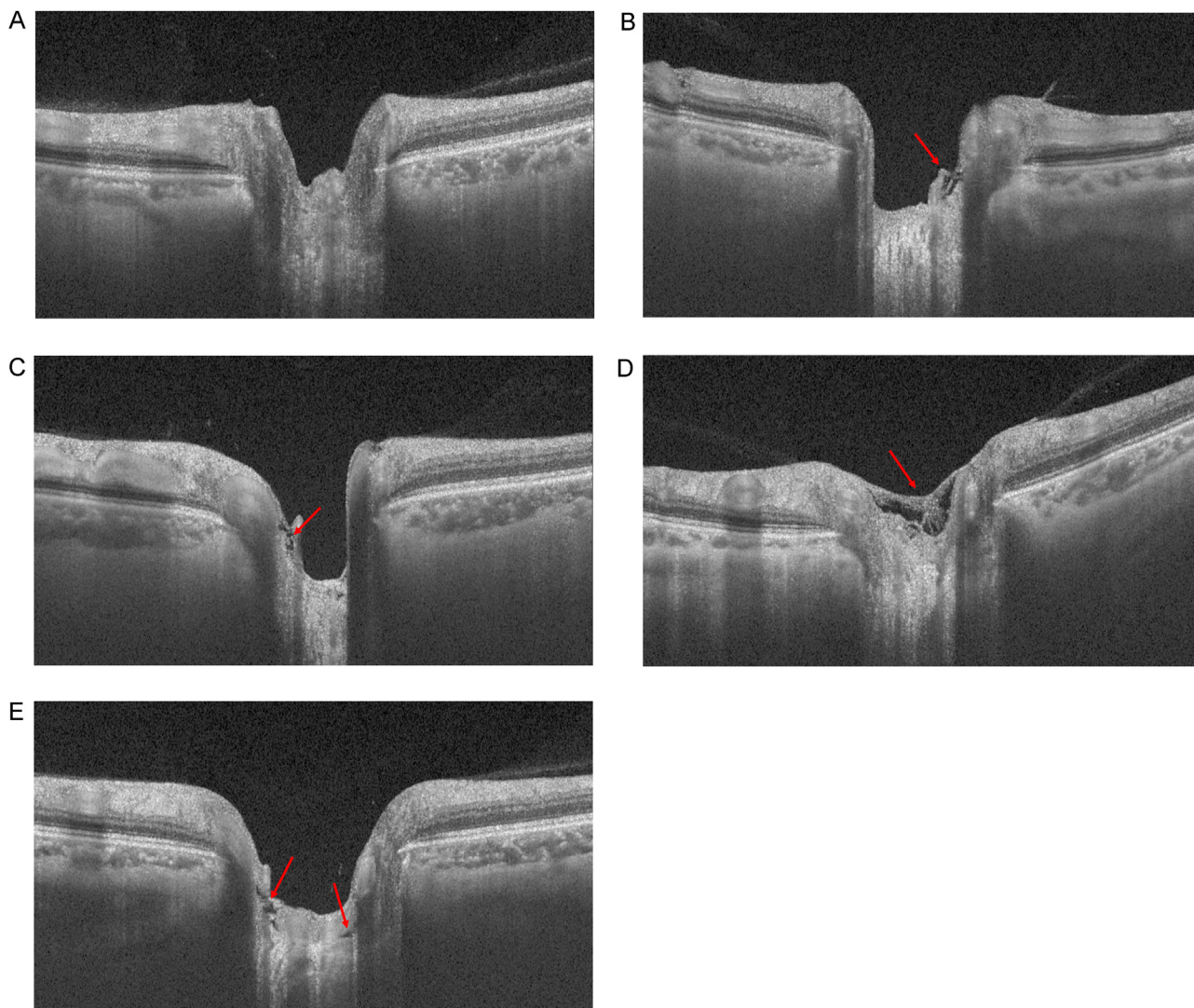


FIGURE 2. Grading of prelaminar schisis. A. Eye with no prelaminar schisis. B, C. Eyes with grade 1 prelaminar schisis. Red arrows point to locations of separation of ILM and separating of vessels from the prelaminar tissue. D, E. Eyes with grade 2 prelaminar schisis. Red arrows point to more extensive and deeper detachment of prelaminar tissues as well as the lifting of vessels.

posterior vitreous membrane without detachment, and perifoveal PVD with persistent adhesion of the posterior vitreous to the papilla and fovea were considered to have early-stage PVD (stage 0, 1a, 1b, 2 of Tsukahara et al¹⁸). Eyes with perifoveal and peripapillary PVD with persistent adhesion of the posterior vitreous to the papilla and complete PVD in both the perifoveal and peripapillary region were considered to have late-stage PVD (stage 3, 4 of Tsukahara et al¹⁸). Eyes with no visible posterior vitreous membrane upon the OCT images (13 normal eyes and 12 glaucomatous eyes) were clinically judged to have complete PVD because the premacular bursa and area of Martegiani were invisible and all were over the age of 50 years.

• **DETERMINATION OF BERGMEISTER PAPILLA ON OCT SCANS:** The presence of Bergmeister papilla was deter-

mined on the ONH raster scans as a tissue structure embedded in the rim of the ONH extending into the vitreous.^{19,20} (Figure 3, A and B)

• **STATISTICAL ANALYSIS:** Statistical analyses were performed with IBM SPSS version 27 (IBM Corp.). Differences between normal and glaucomatous eyes were evaluated using unpaired 2-sided *t* tests for continuous variables or by Fisher exact tests for categorical variables. Intra- and interobserver repeatability of the presence and severity of PLS were calculated by Cohen kappa coefficients and Cohen weighted kappa coefficients.

To explore factors associated with the severity of PLS, a univariate analysis was first conducted with the following explanatory variables: age, AXL, IOP at time of OCT image acquisition, BMO area, BMO ovality, ASCO area, ASCO

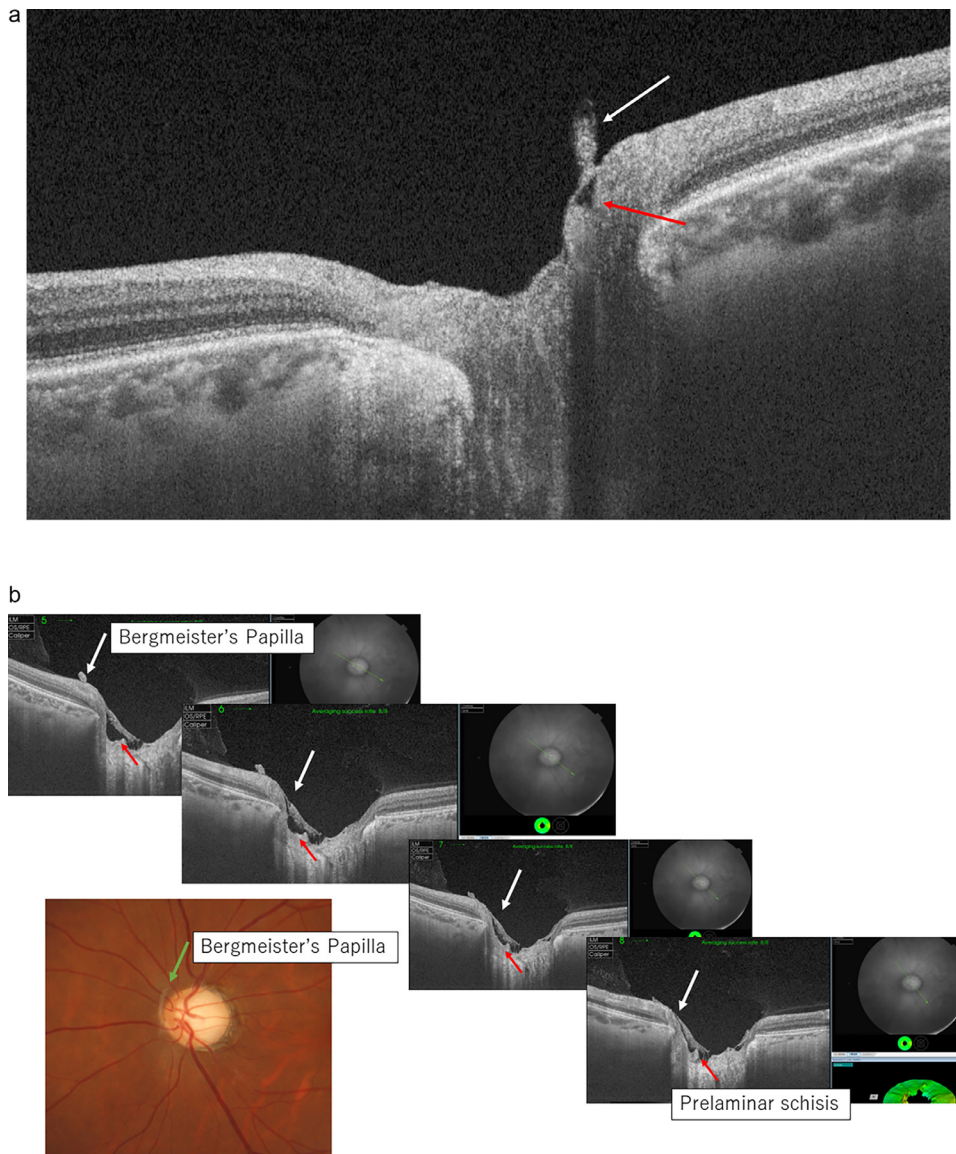


FIGURE 3. A. Eye with Bergmeister papilla on the nasal inferior region of the optic disc (white arrow) and a prelaminar schisis right below the Bergmeister papilla (red arrow). **B.** Eye with Bergmeister's papilla that can be observed on optic disc photograph (green arrow). Bergmeister papilla (white arrows) and prelaminar schisis (red arrows) can be seen upon the OCT scans.

ovality, ASCO/BMO offset magnitude, ASCO/BMO offset direction, PPA+BM, PPA-BM, MRW, cpRNFLT, cpChT, LCD, LC-GSI and PPS angle, PVD staging (early/late), presence of Bergmeister papilla, and mean deviation (MD) of the 24-2 SITA-standard HFA results (glaucomatous eyes only). Next, a multivariable proportional odds logistic regression analysis was conducted including age, variables that achieved P values of $<.2$ upon univariate analysis, and variables reported to be associated with PLS (BMO area,⁶ MRW,⁶ LCD,⁷ AXL²¹). ASCO/BMO offset magnitude and PPA-BM were strongly correlated with each other ($R = 0.800$, $P < .0001$ ¹³). We included ASCO/BMO offset magnitude in our multivariable model because the univariate model with ASCO/BMO offset mag-

nitude demonstrated a better fit ($P < .001$, likelihood test).

RESULTS

Data for 230 eyes of 155 normal subjects and 157 eyes of 122 glaucomatous patients who met the inclusion criteria were collected. After excluding 25 normal eyes and 15 glaucomatous eyes because of LC and scleral segmentation errors and randomly selecting one eye of each participant, 110 eyes of 110 normal subjects and 107 eyes of 107 glaucomatous patients were enrolled in the study. There was excellent

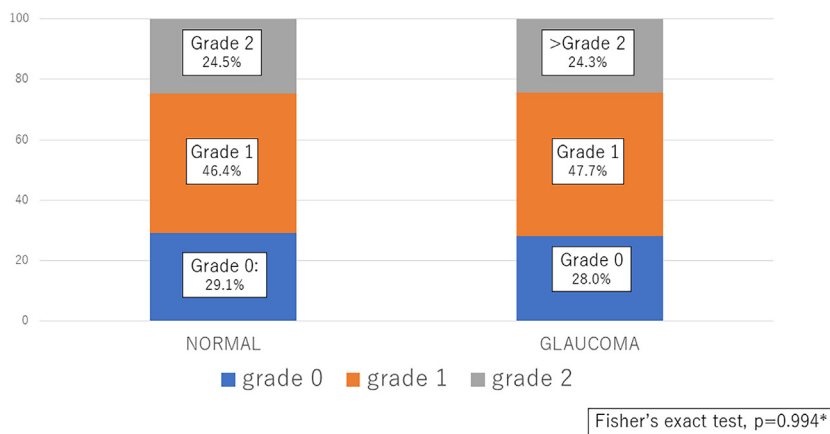


FIGURE 4. Frequency and severity of prelamellar schisis in normal and glaucomatous eyes. There was no difference in frequency or severity between normal and glaucomatous eyes. (Fisher exact test, $P = .882$ and $P = 0.994$, respectively).

intra- and inter-reproducibility for presence of PLS (Cohen $\kappa = 0.918, 0.915$) as well as severity of PLS (Cohen weighted $\kappa = 0.885, 0.885$).

Comparison of baseline characteristics and ONH parameters between the normal and glaucomatous eyes and between eyes with and without PLS are presented in Table 2. There was no difference in age or AXL among the groups. Frequency of Bergmeister papilla was significantly higher in eyes with PLS for both normal and glaucomatous eyes ($P < .001$).

Among the normal eyes, 32 eyes (29.1%) had no PLS, 51 (46.4%) had grade 1 PLS, and 27 (24.5%) had grade 2 PLS. Among the glaucomatous eyes, 30 (28.0%) had no PLS, 51 (47.7%) had grade 1 PLS, and 26 (24.3%) had grade 2 PLS. The frequency and severity of PLS did not differ between normal and glaucomatous eyes ($P = .882, .994$, respectively) (Figure 4).

The presence of Bergmeister papilla was the strongest predictor of a more severe PLS in both normal eyes (odds ratio [OR] = 9.81, $P < .001$) and glaucomatous eyes (OR = 20.56, $P < .001$). A larger PPS angle in normal eyes (OR = 1.18, $P = .005$) and larger BMO area (OR = 1.09, $P = .032$) and deeper LCD in glaucomatous eyes (OR = 1.06, $P = .036$) were also associated with PLS severity Tables 3 and 4.

DISCUSSION

In the current study, the overall frequency of PLS (normal: 70.9%, glaucoma: 72%) was higher than the 42% reported for normal and mild glaucomatous eyes⁶ and 41% reported for advanced glaucomatous eyes.⁷ The reported frequency of PLS greater than grade 2 in glaucomatous eyes (~20%) was similar to our 24.3%, suggesting that our overall higher frequency of PLS was driven mainly by the detection of subtler grade 1 changes. One reason for this discrepancy in

overall frequency may be attributed to the use of SS-OCT as opposed to the use of spectral domain OCT (Spectralis, Heidelberg Engineering).^{6,7}

Both the frequency and severity of PLS were not different between the normal and glaucomatous eyes in our study. Furthermore, indices measuring glaucoma severity such as MD of HFA results, MRW, and cpRNFLT were all not associated with severity of PLS, suggesting that mild-to-moderate PLS may not be a glaucoma-related finding. These results are discrepant with an earlier study that reported PLS to be observed more frequently in glaucomatous eyes than in normal eyes (33.0% vs 44.6%).⁶ However, the small number of grade 3 PLS eyes in our cohort limited the power of our study to explore the relationship between glaucomatous damage and extensive splitting of the prelamellar region. The fact that the three grade 3 PLS eyes were all glaucomatous eyes was in agreement with the previous report,⁶ which may imply that a more severe form of PLS is associated with glaucomatous damage.

We found a higher frequency of grade 2 PLS in normal eyes in comparison to previous reports, resulting in no statistical difference between the 2 groups of our study. Lamina cribrosa morphology has been reported to differ among races,²² and the large proportion of Asian subjects in our study cohort (>90%) may have had an impact on our results. Temporal structure–function discordance may be another reason for this discrepancy. Peripapillary retinoschisis, a similar splitting of the retinal tissues in the peripapillary region, was reported to have no impact on short-term visual field sensitivity,²³ but its presence or increase is purported to be associated with long-term visual field progression.^{8,9} Analogous temporal relationships may be possible with PLS.

Prior studies have proposed that PLS may be a phenomenon caused by the detachment of blood vessels and intra-disc ILM/meniscus of Kuhnt from the underlying prelamellar tissue as glaucomatous damage progresses and ONH cupping becomes deeper. This hypothesis was not

TABLE 2. Comparison of Baseline Characteristics of Study Subjects

Characteristic	Normal	Glaucoma	P Value Normal vs Glaucoma	Normal		P Value Without PLS vs With PLS	Glaucoma		P Value Without PLS vs With PLS
				Eyes Without PLS	Eyes With PLS		Eyes Without PLS	Eyes With PLS	
No. of subjects	110	107		32	78		30	77	
Sex	M: 52 F: 58	M: 40 F: 67	^a 0.141	M: 15 F: 17	M: 37 F: 41	^a 0.957	M: 14 F: 16	M: 26 F: 51	^a 0.309
R/L	R: 63 L: 47	R: 55 L: 52	^a 0.385	R: 15 L: 17	R: 48 L: 30	^a 0.158	R: 19 L: 11	R: 36 L: 41	^a 0.123
Age, y	49.4±9.0 (31-70)	50.7±9.3 (31-70)	0.294	49.1±8.1	49.5±9.4	0.768	49.3±9.4	51.3±9.3	0.272
IOP (mm Hg)	13.9±2.4 (8-20)	13.7±2.4 (9-20)	0.614	14.3±2.2	13.7±2.4	0.300	13.9±2.2	13.7±2.5	0.706
SE (D)	-3.67±2.48	-4.65±3.02	0.013^b	-3.66±2.61	-3.67±2.45	0.858	-5.14±2.78	-4.46±3.10	0.375
AXL (mm)	25.07±1.08 (22.20~27.41)	25.35±1.40 (22.37-27.97)	0.102	25.0±1.12	25.1±1.06	0.739	25.7±1.4	25.2±1.4	0.123
MD (dB)	-0.26±1.19 (-3.42~2.29)	-4.91±3.40 (-11.83~2.28)	<0.001^b	-0.25±1.26	-0.27±1.17	0.530	-5.14±3.36	-4.82±3.44	0.562
BMO area (mm ²)	2.19±0.52	2.57±0.69	<0.001^b	2.04±0.56	2.24±0.49	0.361	2.53±0.65	2.59±0.71	0.729
BMO ovality	1.11±0.08	1.11±0.06	0.411	1.11±0.06	1.12±0.08	0.345	1.10±0.07	1.11±0.06	0.975
ASCO area (mm ²)	2.84±0.57	3.06±0.71	0.015^b	2.71±0.50	2.89±0.59	0.183	2.97±0.72	3.09±0.71	0.512
ASCO ovality	1.15±0.13	1.16±0.12	0.572	1.14±0.11	1.15±0.14	0.646	1.18±0.17	1.15±0.10	0.301
ASCO/BMO offset magnitude (μm)	271.5±159.1	294.5±172.1	0.310	285.1±159.1	263.4±158.8	0.414	336.3±182.4	278.2±166.2	0.100
ASCO/BMO offset direction (°)	165.8±43.4	168.1±39.4	0.685	167.1±47.4	165.2±42.3	0.802	167.1±28.7	168.5±43.1	0.883
Average MRW (μm)	297.4±47.9	196.8±49.2	<0.001^b	315.3±55.2	290.8±43.1	0.035	206.8±51.2	193.0±48.2	0.135
cpRNFLT (μm)	106.0±9.9	81.1±14.7	<0.001^b	106.1±11.2	106.0±9.4	0.912	79.1±11.2	81.9±15.8	0.424
cpCHT (μm)	127.9±52.1	118.1±49.7	0.158	123.8±39.0	130.0±56.9	0.355	123.7±55.6	115.9±47.5	0.254
PPA+BM area (mm ²)	0.83±0.64	0.97±0.43	0.072	0.85±0.53	0.83±0.69	0.764	0.91±0.34	0.99±0.46	0.400
PPA-BM area (mm ²)	0.29±0.34	0.42±0.36	0.010^b	0.30±0.39	0.28±0.32	0.334	0.50±0.38	0.39±0.35	0.146
LC depth (μm)	412.2±98.1	458.7±104.9	<0.001^b	388.1±80.1	422.5±103.5	0.076	451.1±101.5	461.7±106.7	0.800
LC-global shape index	-0.77±0.22	-0.80±0.19	0.327	-0.72±0.27	-0.78±0.20	0.153	-0.76±0.25	-0.81±0.16	0.180
Peripapillary scleral angle (°)	7.36±4.38	10.31±4.38	<0.001^b	5.76±3.90	8.00±4.44	0.019	10.06±4.81	10.41±4.23	0.567
Late-stage PVD	20.9% (23 eyes)	26.2% (28 eyes)	0.361	21.8% (7 eyes)	20.5% (16 eyes)	0.873	23.3% (7 eyes)	27.3% (21 eyes)	0.864
Bergmeister papilla	78.2% (86 eyes)	75.7% (81 eyes)	0.188	50.0% (16 eyes)	89.7% (70 eyes)	<0.001^b	40.0% (12 eyes)	89.6% (69 eyes)	<0.001^b

ASCO = anterior scleral canal opening; AXL = axial length; BMO = Bruch membrane opening; cpChT = circumpapillary choroidal thickness; cpRNFLT = circumpapillary retinal nerve fiber layer thickness; D = diopter; F = female; IOP = intraocular pressure; L = left; LC = lamina cribrosa; M = male; MD = mean deviation; MRW = minimum rim width; PLS = prelaminar schisis; PPA = peripapillary atrophy; PVD = posterior vitreous detachment; R = right; SE = spherical equivalent.

^aP values from χ^2 test; all other P values from unpaired t test.

^bStatistically significant P values after correction by Benjamini-Hochberg procedure with false discovery rates set at 5%. Values shown as average ± SD.

TABLE 3. Univariate and Multivariate Ordinal Logistic Regression Models for Factors Predicting the Severity of Prelaminar Schisis in Normal Eyes.

Characteristic	Increment	Univariate Analysis		Multivariate Analysis	
		Odds ratio (95% CI)	<i>P</i> Value	Odds Ratio (95% CI)	<i>P</i> Value
Age	10 y older	0.98 (0.67-1.45)	0.938	0.89 (0.55-1.45)	0.640
AXL (mm)	1 mm longer	1.02 (0.74-1.41)	0.915	0.70 (0.43-1.17)	0.174
Late-stage PVD	TRUE	1.16 (0.49-2.73)	0.741	1.16 (0.39-3.46)	0.795
Bergmeister's papilla	TRUE	9.98 (3.68-27.9)	<0.001	9.81 (3.39-28.4)	<0.001
BMO area (mm ²)	0.1 mm ² larger	1.05 (0.98-1.12)	0.192	1.08 (0.99-1.19)	0.090
BMO ovality	0.1 larger	1.44 (0.90-2.32)	0.130	1.31 (0.77-2.20)	0.318
ASCO ovality	0.1 larger	1.26 (0.94-1.70)	0.122	1.24 (0.86-1.78)	0.247
cpChT (μm)	10 μm thicker	1.05 (0.98-1.12)	0.199	1.09 (0.97-1.22)	0.160
LC depth (μm)	10 μm deeper	1.02 (0.99-1.06)	0.183	0.99 (0.93-1.05)	0.711
Peripapillary scleral angle (°)	1 degree larger	1.09 (1.01-1.19)	0.037	1.18 (1.05-1.32)	0.005
Average MRW (μm)	10 μm thinner	1.05 (0.97-1.13)	0.238	1.02 (0.92-1.14)	0.676
IOP (mm Hg)	1 mm Hg higher	0.57 (0.82-1.10)	0.455		
ASCO area (mm ²)	0.1 mm ² larger	1.00 (0.95-1.07)	0.877		
ASCO/BMO offset magnitude (μm)	10 μm larger	1.00 (1.00-1.00)	0.416		
ASCO/BMO offset direction (°)	1 degree larger	1.00 (0.99-1.01)	0.690		
PPA+BM area (mm ²)	0.1 mm ² larger	1.01 (0.95-1.06)	0.815		
PPA-BM area (mm ²)	0.1 mm ² larger	1.00 (0.90-1.10)	0.956		
cpRNFLT (μm)	10 μm thinner	1.12 (0.78-1.60)	0.532		
LC-global shape index	0.1 larger	1.00 (0.85-1.17)	0.993		

ASCO = anterior scleral canal opening; AXL = axial length; BMO = Bruch membrane opening; cpChT = circumpapillary choroidal thickness; cpRNFLT = circumpapillary retinal nerve fiber layer thickness; LC = lamina cribrosa; MRW = minimum rim width; PPA = peripapillary atrophy; PVD = posterior vitreous detachment; Statistically significant *P* values presented in boldface type.

TABLE 4. Univariate and Multivariate Ordinal Logistic Regression Models for Factors Predicting the Severity of Prelaminar Schisis in Glaucomatous Eyes.

Characteristic	Increment	Univariate Analysis		Multivariate Analysis	
		Odds Ratio (95% CI)	P Value	Odds Ratio (95% CI)	P Value
Age	10 y older	1.20 (0.82-1.76)	.353	1.07 (0.60-1.90)	.820
AXL (mm)	1 mm longer	0.76 (0.59-0.99)	.039	0.76 (0.51-1.14)	.182
Late stage PVD	TRUE	1.14 (0.51-2.56)	.749	1.09 (1.01-1.17)	.784
Bergmeister's papilla	TRUE	14.51 (5.21-40.45)	<.001	20.56 (6.58-64.22)	<.001
BMO area (mm²)	0.1 mm² larger	1.00 (0.95-1.05)	.908	1.09 (1.01-1.17)	.032
ASCO/BMO offset magnitude (µm)	10 µm larger	0.98 (0.96-1.00)	.029	0.97 (0.94-1.01)	.102
PPA-BM area (mm ²)	0.1 mm ² larger	0.89 (0.81-0.99)	.031		
cpChT (µm)	10 µm thicker	0.99 (0.92-1.06)	.785	0.92 (0.83-1.04)	.181
LC depth (µm)	10 µm deeper	1.00 (0.98-1.04)	.600	1.06 (0.99-1.11)	.036
Average MRW (µm)	10 µm thinner	1.02 (0.95-1.10)	.584	0.94 (0.85-1.04)	.247
IOP (mmHg)	1 mm Hg higher	0.73 (0.84-1.12)	.681		
MD (dB)	1 db more negative	0.97 (0.87-1.08)	.543		
BMO ovality	0.1 larger	1.10 (0.96-1.06)	.753		
ASCO area (mm ²)	0.1 mm ² larger	1.01 (0.86-1.06)	.723		
ASCO ovality	0.1 larger	0.94 (0.70-1.26)	.680		
ASCO/BMO offset direction (°)	1 degree larger	1.00 (0.99-1.01)	.615		
PPA+BM area (mm ²)	0.1 mm ² larger	1.00 (0.92-1.09)	.956		
cpRNFLT (µm)	10 µm thinner	0.90 (0.71-1.15)	.412		
LC-global shape index	0.1 larger	0.90 (0.75-1.09)	.292		
Peripapillary scleral angle (°)	1 degree larger	1.00 (0.92-1.08)	.934		

ASCO = anterior scleral canal opening; AXL = axial length; BMO = Bruch membrane opening; cpChT = circumpapillary choroidal thickness; cpRNFLT = circumpapillary retinal nerve fiber layer thickness; LC = lamina cribrosa; MD = mean deviation; MRW = minimum rim width; PPA = peripapillary atrophy; PVD = posterior vitreous detachment.

Statistically significant P values presented in boldface type.

confirmed with their insignificant association between visual field indices and the presence of or severity of PLS, although structure–function discordance must be taken into consideration in cross-sectional studies with constricted stages of glaucomatous damages. Furthermore, despite the implications of association of vitreo-retinal traction with the presence of PLS,⁷ a thorough assessment of the vitreous was not conducted in both studies because of the use of enhanced depth image SD-OCT, which sacrifices the resolution quality of the inner retinal layers and vitreous region for better visibility of the deeper ONH structures.²⁴ Our use of SS-OCT enabled deeper light penetration with less variability in sensitivity,²⁵ and better visibility of the prelaminar and lamellar region as well as the vitreous region for the purposes of our study.^{11,25,26}

Multivariable logistic models revealed that the presence of Bergmeister papilla was the only parameter significantly associated with the severity of PLS in both normal and glaucomatous eyes ($P < .001$). Bergmeister papilla is a residue of the hyaloid artery that nourishes the lens through the Cloquet canal, which can be observed as an epipapillary veil consisting of glial/fibrotic/vascular tissue in the intradisc region.²⁷ Bergmeister papilla not visible on funduscopy is known to be discernible on OCT images as a stalk-like reflective structure extending anteriorly from the ONH,¹⁹ and a recent study in children revealed that the prevalence of SS-OCT–detected Bergmeister papilla was 67.8%.²⁰ Although Bergmeister papilla is generally considered to be a benign condition commonly observed in normal eyes, its association with tractional diseases including vitreous hemorrhages, tractional retinal detachment, or macular hole has been previously reported.²⁸⁻³⁰ A milder contraction of the fibro-vascular mass may exert tangential traction on the inner retinal layers of the ONH, resulting in a splitting or lifting of the ILM/meniscus of Kuhnt within the optic disc excavation.

A recent case report³¹ presented an OCT image of an optic disc with Bergmeister papilla demonstrating a typical splitting of the prelaminar tissue as observed in PLS. Two representative cases indicative of association between Bergmeister papilla and PLS from our dataset are presented in Figure 3, A and B. Over 90% of the Bergmeister papillae in our dataset were visible only on OCT images, in agreement with previous reports.²⁰ Bergmeister papilla observed on OCT images were observed mainly (81.1%) on the nasal or nasal inferior side of the ONH, although continuity between Bergmeister papilla and PLS was not necessarily observed.

Staging of PVD was not selected as a predictor of PLS in our multivariable analysis ($P \geq .6$). Most of the eyes with PLS (79.4%) were still in the earlier stages of PVD, suggesting that traction from the posterior vitreous membrane is unlikely to exert a strong impact on prelaminar tissue splitting (Supplemental Figure).

A larger PPS angle indicating a more posteriorly bowed PPS was also associated with PLS severity in normal eyes.

A more posteriorly bowed PPS may enhance the tractional forces on the inner surface of the ONH cup of normal eyes, leading to a more severe PLS. However, evaluation of peripapillary structure on OCT B-scans needs to be interpreted with caution. OCT B-scans have been shown to present distorted versions of the ocular posterior segment morphology, and it has been found that angles measured upon the B-scans do not necessarily reflect the true dimensions of the ocular globe.³² Furthermore, distortion proportion changes with AXL,³³ which makes correction for this distortion very difficult. Although AXL was taken into consideration in our multivariable analysis, correction may be insufficient because the precise relationship between distortion proportion and AXL is still unknown. However, as our PPS boundary was measured on a relatively short distance of 600 μm (Figure 1), the degree of distortion is expected to be minimal, and a comparison of OCT image–measured angles should still be able to reveal relative variations among the images. Further elucidation of relationships between PPS structure and the development of PLS should await future studies.

The association of a larger BMO area and a deeper LCD with the severity of PLS in glaucomatous eyes were in agreement with previous reports.^{6,7} Taken together with the fact that larger PPS angle,¹⁶ larger BMO area,⁶ and deeper LCD³⁴ are all known to be associated with glaucoma, our results suggest possible association between severity of PLS and the glaucomatous damaging process. Future studies with enrollment of larger number of subjects, including those with advanced glaucomatous eyes, would be beneficial to confirm this relationship.

Previous studies have reported the presence of PLS in pathologically myopic eyes,³⁵ as well as an association with shorter AXL and PLS in advanced glaucomatous eyes,⁷ suggesting some relationship between AXL and PLS. Although the relationship between extremely long AXL and PLS is unclear because the frequency of PLS was not compared to non–pathologically myopic eyes in the previous study, there is a possibility that the results of our study would have differed if pathologically myopic eyes had been included. However, we consider pathological myopia to be an entity different from healthy myopic AXL elongation. Our study focused on the evaluation of PLS in non–pathologically myopic normal and mild-to-moderate glaucoma eyes, which is of interest because the great majority of eyes fall into this category. One speculation for the association between short AXL and PLS is that posterior vitreous traction may already be weak at the timing of optic disc cupping in eyes with longer AXL due to early liquefaction of the posterior hyaloid. However, AXL was not selected as an associating factor for the severity of PLS in both the normal and glaucomatous eyes of our dataset. Furthermore, the fact that PVD staging was not the cause for PLS in most of our cases supports our result that AXL was not associated with a more severe PLS. However, an association with shorter AXL and Bergmeister papilla has been reported in healthy

children,²⁰ and there could be a possible indirect relationship among AXL, the presence of Bergmeister papilla, and PLS.

There are several limitations that may affect the results of our study. The relatively small number of subjects included in our study may have limited the detection of more severe PLS. The cross-sectional nature of our study is another limitation. There is a possibility that prelamellar schisis is a congenital condition in which the prelamellar tissues did not complete their growth to fill that area, as also seen in optic nerve colobomas, or that PLS is a constantly changing and/or transient finding as is reported with peripapillary retinoschisis.³⁶ Future longitudinal studies will be needed to elucidate the true relationship between traction on the ONH and development of PLS, as well as its relationship with functional loss. Analysis of baseline IOP and prelamellar schisis severity was not possible because of the lack of pretreatment information. However, con-

sidering the high proportion of normal-tension glaucoma (NTG) in the Asian population,³⁷ our cohort was most likely constituted mainly of NTG subjects. Finally, the use of the BMO plane as a reference for measurement of LCD is known to be affected by age and choroidal thickness.³⁸ Thus, we corrected for both effects of age and cpChT in our analysis.

In conclusion, our results demonstrate that mild to moderate PLS was strongly associated with the presence of Bergmeister papilla, suggesting the involvement of a traction-related phenomenon. However, the correlation of PLS and posteriorly bowed peripapillary scleral configuration in normal eyes and larger BMO area and deeper LCD in glaucomatous eyes may suggest a possible association with glaucomatous structural changes, which warrants future studies on the relationship between the development of PLS and the extent of glaucomatous damage.

Funding/Support: Support was provided by the following: Topcon and Japan Society for the Promotion of Science (Project number: 20K18368) (H.S.); Council for Science, Technology and Innovation (CSTI), Cross-ministerial Strategic Innovation Promotion Program (SIP) "Innovative AI Hospital System (A.M.); Topcon (C.K.S.L., T.-W.K., L.Z., R.W.); National Eye Institute EY027510 (L.Z.). Financial Disclosures: Carl Zeiss Meditec, Topcon, Senju, Otsuka, Santen, Kowa, Novartis, Abbvie, Viartis (Honoraria) (H.S.); Santen, Alcon Japan, Senju, Bayers (Honoraria) (T.U.); Pfizer, Santen, Topcon, Senju, Aerie, Kowa (Consultants), Pfizer, Senju, Kowa (Honoraria), GSTK-DiscAnalysis (License) (M.A.); Kowa, Beeline (Royalties) (H.M.); Topcon (employee) (T.K.); Santen, Otsuka, Senju, Kowa, Novartis, Viartis, Bayers, Inami Company (Honoraria) (K.S.); Allergan Japan, Bayer, HOYA, Kowa, Nitto Medic, Novartis, Otsuka, Pfizer, Santen, Senju, Viartis (Honoraria) (T.H.); Alcon, Ellex, Kowa, Menicon, Nitten, Nitto Medic, Otsuka, Rohto, SEED, Senju, Viartis, Topcon (Honoraria), Santen (Consultant) (A.M.); Topcon Corp (Patent), Carl Zeiss Meditec, CREWT Medical Systems, Heidelberg Engineering, Santen, Senju, Otsuka, Novartis (Honoraria) Santen (Consultant) (A.I.); Senju, Viartis, Nitto Medic (Honoraria) (G.T.); Topcon Corp, Nidek, Senju (Grants), Topcon Corp, Nidek, Senju (Honoraria) (T.N.); Santen, CooperVision (Consultant) (K.O.-M.); Santen, Alcon, Pfizer, Otsuka, HOYA, TOMEY, CREWT Medical systems, Carl Zeiss Meditec, Senju, Novartis, Kowa, Johnson & Johnson, Glaukos, Iridex, Canon (Honoraria) Santen, Alcon, Pfizer, Otsuka, Johnson & Johnson, TOMEY, CREWT medical systems, Senju, Novartis, Kowa, Wakamoto, Glaukos, Ono, Sato (Grants) Santen, Alcon, Kowa, Wakamoto, Glaukos, Astellas, Senju, Pfizer, Otsuka, HOYA, IRIDEX (Consultant) Santen, HOYA, Senju, Kowa (Advisory Board) (M.A.); Carl Zeiss Meditec (Licenses), Topcon, Santen (Honoraria), Santen, Janssen (Advisory Board), Carl Zeiss Meditec, Heidelberg Engineering (Equipment loan) (C.K.S.L.); Heidelberg Engineering, Carl Zeiss Meditec (Grants), Carl Zeiss Meditec (License), Abbvie, Digital Diagnostics (Consultants), Topcon, Optovue, Heidelberg Engineering, Carl Zeiss Meditec (Research instruments) (L.Z.); Consultant: Abbvie, Aerie Pharmaceuticals, Alcon, Allergan, Amydis, Editas, Equinox, Eyeovia, Iantrek, Implandata, IOPtic, iStar Medical, Nicox, Santen, Topcon; Research Support: National Eye Institute, National Institute of Minority Health and Health Disparities; Research Instruments: Heidelberg Engineering, Topcon, Zeiss Meditec, Optovue, Centervue, Zilia; Patents (licensed by UCSD), Zeiss Meditec, Toromedes (R.N.W.). None of the other authors report financial disclosures or conflicts of interest. All authors attest that they meet the current ICMJE criteria for authorship.

REFERENCES

1. Quigley HA, Addicks EM, Green WR, Maumenee AE. Optic nerve damage in human glaucoma. II. The site of injury and susceptibility to damage. *Arch Ophthalmol*. 1981;99(4):635–649. doi:10.1001/archophth.1981.03930010635009.
2. Miller KM, Quigley HA. The clinical appearance of the lamina cribrosa as a function of the extent of glaucomatous optic nerve damage. *Ophthalmology*. 1988;95(1):135–138. doi:10.1016/s0161-6420(88)33219-7.
3. Quigley HA, Hohman RM, Addicks EM, Massof RW, Green WR. Morphologic changes in the lamina cribrosa correlated with neural loss in open-angle glaucoma. *Am J Ophthalmol*. 1983;95(5):673–691. doi:10.1016/0002-9394(83)90389-6.
4. Tezel G, Trinkaus K, Wax MB. Alterations in the morphology of lamina cribrosa pores in glaucomatous eyes. *Br J Ophthalmol*. 2004;88(2):251–256. doi:10.1136/bjo.2003.019281.
5. Fortune B. Pulling and tugging on the retina: mechanical impact of glaucoma beyond the optic nerve head. *Invest Ophthalmol Vis Sci*. 2019;60(1):26–35. doi:10.1167/iovs.18-25837.
6. Lowry EA, Mansberger SL, Gardiner SK, et al. Association of optic nerve head prelamellar schisis with glaucoma. *Am J Ophthalmol*. 2021;223:246–258. doi:10.1016/j.ajo.2020.10.021.
7. Sung MS, Jin HN, Park SW. Clinical features of advanced glaucoma with optic nerve head prelamellar schisis. *Am J Ophthalmol*. 2021;232:17–29. doi:10.1016/j.ajo.2021.06.007.
8. Fortune B, Ma KN, Gardiner SK, Demirel S, Mansberger SL. Peripapillary retinoschisis in glaucoma: association with progression and oct signs of müller cell involvement. *Invest Ophthalmol Vis Sci*. 2018;59(7):2818–2827. doi:10.1167/iovs.18-24160.
9. Lee EJ, Kee HJ, Han JC, Kee C. The progression of peripapillary retinoschisis may indicate the progression of glaucoma. *Invest Ophthalmol Vis Sci*. 2021;62(2):16. doi:10.1167/iovs.62.2.16.
10. Ohno-Matsui K, Shimada N, Yasuzumi K, et al. Long-term development of significant visual field defects in highly myopic

- eyes. *Am J Ophthalmol*. 2011;152(2):256–265. doi:10.1016/j.ajo.2011.01.052.
11. Lavinsky F, Lavinsky D. Novel perspectives on swept-source optical coherence tomography. *Int J Retina Vitreous*. 2016;2:25. doi:10.1186/s40942-016-0050-y.
 12. Hodapp E, Parrish R, Anderson DR. *Clinical Decisions in Glaucoma*. 1993.
 13. Saito H, Kambayashi M, Araie M, et al. Deep optic nerve head structures associated with increasing axial length in healthy myopic eyes of moderate axial length. *Am J Ophthalmol*. 2023;249:156–166. doi:10.1016/j.ajo.2023.01.003.
 14. Littmann H. Zur Bestimmung der wahren Größe eines Objektes auf dem Hintergrund eines lebenden Auges [Determining the true size of an object on the fundus of the living eye]. *Klin Monbl Augenheilkd*. 1988;192(1):66–67. doi:10.1055/s-2008-1050076.
 15. Thakku SG, Tham YC, Baskaran M, et al. A global shape index to characterize anterior lamina cribrosa morphology and its determinants in healthy Indian eyes. *Invest Ophthalmol Vis Sci*. 2015;56(6):3604–3614. doi:10.1167/iops.15-16707.
 16. Wang X, Tun TA, Nongpiur ME, et al. Peripapillary sclera exhibits a v-shaped configuration that is more pronounced in glaucoma eyes. *Br J Ophthalmol*. 2020. doi:10.1136/bjophthalmol-2020-317900.
 17. Liu JJ, Witkin AJ, Adhi M, et al. Enhanced vitreous imaging in healthy eyes using swept source optical coherence tomography. *PLoS One*. 2014;9(7):e102950. doi:10.1371/journal.pone.0102950.
 18. Tsukahara M, Mori K, Gehlbach PL, Mori K. Posterior vitreous detachment as observed by wide-angle OCT imaging. *Ophthalmology*. 2018;125(9):1372–1383. doi:10.1016/j.ophtha.2018.02.039.
 19. Kagemann L, Wollstein G, Ishikawa H, et al. Persistence of Cloquet's canal in normal healthy eyes. *Am J Ophthalmol*. 2006;142(5):862–864. doi:10.1016/j.ajo.2006.05.059.
 20. Lin Q, Deng J, Ohno-Matsui K, He X, Xu X. The existence and regression of persistent Bergmeister's papilla in myopic children are associated with axial length. *Transl Vis Sci Technol*. 2021;10(13):4. doi:10.1167/tvst.10.13.4.
 21. Han JC, Han SH, Park DY, Lee EJ, Kee C. Clinical course and risk factors for visual field progression in normal-tension glaucoma with myopia without glaucoma medications. *Am J Ophthalmol*. 2020;209:77–87. doi:10.1016/j.ajo.2019.08.023.
 22. Girkin CA, Fazio MA, Bowd C, et al. Racial differences in the association of anterior lamina cribrosa surface depth and glaucoma severity in the African Descent and Glaucoma Evaluation Study (ADAGES). *Invest Ophthalmol Vis Sci*. 2019;60(13):4496–4502. doi:10.1167/iops.19-26645.
 23. Kim JA, Lee EJ, Kim TW. Impact of peripapillary retinoschisis on visual field test results in glaucomatous eyes. *Br J Ophthalmol*. 2022. doi:10.1136/bjophthalmol-2021-320509.
 24. Spaide RF, Koizumi H, Pozzoni MC. Enhanced depth imaging spectral-domain optical coherence tomography. *Am J Ophthalmol*. 2008;146(4):496–500. doi:10.1016/j.ajo.2008.05.032.
 25. Potsaid B, Baumann B, Huang D, et al. Ultrahigh speed 1050nm swept source/Fourier domain OCT retinal and anterior segment imaging at 100,000 to 400,000 axial scans per second. *Opt Express*. 2010;18(19):20029–20048. doi:10.1364/oe.18.020029.
 26. Girard MJ, Tun TA, Husain R, et al. Lamina cribrosa visibility using optical coherence tomography: comparison of devices and effects of image enhancement techniques. *Invest Ophthalmol Vis Sci*. 2015;56(2):865–874. doi:10.1167/iops.14-14903.
 27. Bedell AJ, Jokl A. Epipapillary tissues. *Trans Am Ophthalmol Soc*. 1954;52:291–304.
 28. Gandorfer A, Rohleder M, Charteris D, Kampik A, Luthert P. Ultrastructure of vitreomacular traction syndrome associated with persistent hyaloid artery. *Eye (Lond)*. 2005;19(3):333–336. doi:10.1038/sj.eye.6701459.
 29. Sundararajan M, Jansen ME, Gupta M. Unilateral persistence of the hyaloid artery causing vitreopapillary and vitreomacular traction. *JAMA Ophthalmol*. 2018;136(5):e180221. doi:10.1001/jamaophthalmol.2018.0221.
 30. Delaney Jr WV. Prepapillary hemorrhage and persistent hyaloid artery. *Am J Ophthalmol*. 1980;90(3):419–421. doi:10.1016/s0002-9394(14)74928-1.
 31. Jain P PA, Shinde P. An insight on Bergmeister's papillae. *Indian J Ophthalmol Case Rep*. 2022;2:277–278. doi:10.4103/ijoo.IJO_849_21.
 32. Kuo AN, McNabb RP, Chiu SJ, et al. Correction of ocular shape in retinal optical coherence tomography and effect on current clinical measures. *Am J Ophthalmol*. 2013;156(2):304–311. doi:10.1016/j.ajo.2013.03.012.
 33. McNabb RP, Polans J, Keller B, et al. Wide-field whole eye OCT system with demonstration of quantitative retinal curvature estimation. *Biomed Opt Express*. 2019;10(1):338–355. doi:10.1364/boe.10.000338.
 34. Park SC, Brumm J, Furlanetto RL, et al. Lamina cribrosa depth in different stages of glaucoma. *Invest Ophthalmol Vis Sci*. 2015;56(3):2059–2064. doi:10.1167/iops.14-15540.
 35. Xie S, Kamoi K, Igarashi-Yokoi T, et al. Structural abnormalities in the papillary and peripapillary areas and corresponding visual field defects in eyes with pathologic myopia. *Invest Ophthalmol Vis Sci*. 2022;63(4):13. doi:10.1167/iops.63.4.13.
 36. Dhingra N, Manoharan R, Gill S, Nagar M. Peripapillary schisis in open-angle glaucoma. *Eye (Lond)*. 2017;31(3):499–502. doi:10.1038/eye.2016.235.
 37. Iwase A, Suzuki Y, Araie M, et al. The prevalence of primary open-angle glaucoma in Japanese: the Tajimi Study. *Ophthalmology*. 2004;111(9):1641–1648. doi:10.1016/j.ophtha.2004.03.029.
 38. Luo H, Yang H, Gardiner SK, et al. Factors influencing central lamina cribrosa depth: a multicenter study. *Invest Ophthalmol Vis Sci*. 2018;59(6):2357–2370. doi:10.1167/iops.17-23456.